Progresses on SAR remote sensing of tropical forests: forest biomass retrieval and analysis of changing weather conditions

TEBLDINI Stefano[1], YANG Xinwei [1, 2], BAI Yu [1, 3], MARIOTTI D′ALESSANDRO Mauro[1], LIAO Mingsheng [2], YANG Wen[3]

1. *DEIB, Politecnico di Milano, Milan,* 20133*, Italy*;
2. *LIESMARS, Wuhan University, Wuhan,* 430079*, China*;
3. *School of Electronic Information, Wuhan University, Wuhan,* 430072*, China*

Abstract: This paper is intended to report on the progresses made during the Dragon-4 project Three and Four-Dimensional Topographic Measurement and Validation (ID: 32278), sub-project Multi-baseline SAR Processing for 3D/4D reconstruction (ID: 32278_2). The work here reported focuses on two important aspects of SAR remote sensing of tropical forests, namely the retrieval of forest biomass and the assessment of effects due to changing weather conditions. Recent studies have shown that by using SAR tomography the backscattered power at 30 m layer above the ground is linearly correlated to the forest AGB (Above Ground Biomass). However, the two parameters that determine this linear relationship might vary for different tropical forest sites. For purpose of solving this problem, we investigate the possibility of using LiDAR derived AGB to help training the two parameters. Experimental results obtained by processing data from the TropiSAR campaign support the feasibility of the proposed concept. This analysis is complemented by an assessment of the impact of changing weather conditions on tomographic imaging, for which we simulate BIOMASS repeat pass tomography using ground-based TropiSCAT data with revisit time of 3 days and rainy days included. The resulting backscattered power variation at 30 m are within 1.5 dB. For this forest site, this error is translated into an AGB error of about 50-80 ton/ha, which is 20% or less of forest AGB.

Key words: Tropical forest, biomass, SAR tomography, LiDAR, temporal decorrelation

Citation format: Tebldini S, Yang X W, Bai Y, Mariotti D′Alessandro M, Liao M S and Yang W. 2020. Progresses on SAR remote sensing of tropical forests: forest biomass retrieval and analysis of changing weather conditions. Journal of Remote Sensing(Chinese). 24(S1): 167−172

1 INTRODUCTION

Forest biomass plays an important role in characterizing the global carbon cycle, which acts as an indicator of the global climate change [1-2]. Tropical forests are especially significant as most of the biomass is stored in them. However, the absence of accurate measurements of tropical forest AGB is still a gap to be filled. The 7th Earth Explorer mission BIOMASS was proposed to map the global forest biomass [3]. The fully polarimetric P-band BIOMASS mission will feature tomographic imaging with a revisit time of 3 days during the first year of mission lifetime [4].

The use of P-band SAR Tomography has demonstrated that the backscattered power at 30m is strongly correlated to the forest AGB (Above Ground Biomass) [5-6]. However, how to accurately build the linear equation between AGB and tomographic power without available in-situ measurements is still worth further studying. Moreover, the temporal effect is not fully considered in [5-6], since the data used in the experiments were acquired on the same day and under sunny weather condition.

In this work, we propose to use LiDAR derived AGB to help building the linear relationship between AGB and tomographic power at 30 m. The inversion results are then validated by comparing to in-situ measurements. The impact of changing weather conditions on backscattered power is also analyzed. To achieve this, ground-based TropiSCAT data is used to simulate BIOMASS tomography by taking acquisitions from 7 different days with a temporal sampling of 3 days.

This paper is organized as follows: Section 2 focuses on relating SAR Tomography to tropical forest above ground biomass via LiDAR data. The impact of changing weather conditions on BIOMASS tomography is considered in Section 3. Conclusions are drawn in Section 4.

2 RELATING TOMOGRAPHIC POWER TO TROPICAL FOREST AGB VIA LIDAR DATA

2.1 TROPISAR DATA SET

The TropiSAR campaign was carried out by ONERA in French Guiana in summer 2009, in the frame of Phase A studies for the BIOMASS mission [7]. Six fully polarization SLC images at P-

Received: 2019-10-21; **Accepted:** 2020-04-16

Foundation: Dragon-4 project Three and Four-Dimensional Topographic Measurement and Validation (ID: 32278); sub-project Multi-baseline SAR Processing for 3D/4D reconstruction (ID: 32278_2).

band were acquired by the SETHI airborne radar system during the campaign. The resolutions of the SAR data are 1 m and 1.245 m in slant range and azimuth direction, respectively. The vertical baseline for every two adjacent flights is about 15 m, leading to a vertical resolution about 20 m. Fig. 1 represents the Pauli image of the Paracou test site.

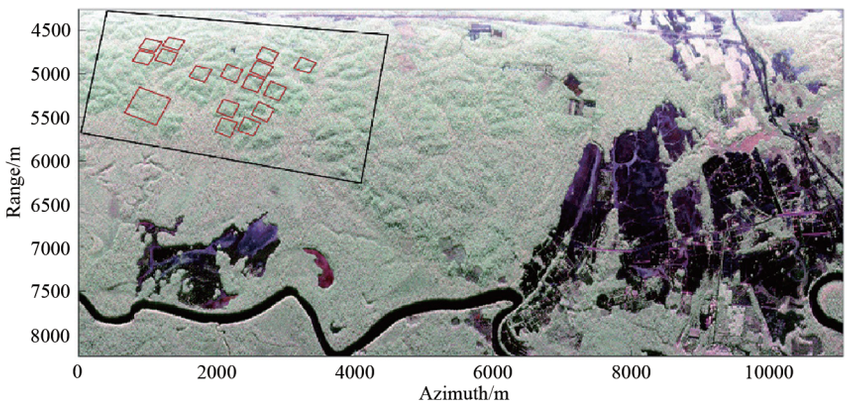

Fig.1 Master image of Paracou test site in Pauli basis. The red squares denote the coverage of in-situ plots while the black square denotes the coverage of LiDAR data.

Since 1984, fifteen permanent 250×250 m^2 plots and one 500×500 m^2 plot have been established, all individual trees with diameter at breast height (DBH) greater than 10 cm were measured for each plot to estimate the AGB. The average AGB of these sixteen plots ranges from 250 ton/ha to 450 ton/ha. Additionally, LiDAR data was also obtained for the test site, which covered all the sixteen in-situ plots. DSM and DTM were generated from the point cloud data by using LAStools and Quick Terrain Modeler at 1 m resolution. The canopy height model (CHM) was afterwards derived by subtracting DTM from DSM, the corresponding AGB map at 0.25 ha scale was finally generated using the CHM.

2.2 SAR BACK-PROJECTION ALGORITHM

SAR tomography is an extension of conventional two-dimensional SAR imaging to three dimensions by building an additional synthetic aperture in elevation direction [8]. It allows a direct localization of multiple scattering contributions within the same slant range-azimuth resolution cell [9]. The standard beamforming algorithm denotes that multi-baseline SAR data and the reflectivity of cross range distribution form a Fourier pair, which can be written as

$$\mathrm{P}(r,x,z)=\left|\frac{1}{\sqrt{N}}\sum_{n=1}^{N}SLC_n(r,x)\,e^{-j\frac{4\pi b_n}{\lambda r}z}\right|^2 \quad (1)$$

Where: o P(r,x,z) is the tomographic backscattered power at range-azimuth location (r, x) and at z meters above the terrain level; o SLC_n(r,x) is the Single-Look-Complex image from the n-th flight; o b_n is the n-th interferometric baseline; o λ is the wavelength.

However, the drawback of beamforming spectral estimation method is that it relies on the linear approximation between interferometric phase and elevation. For this reason, the SAR back-projection algorithm was used in this work to implement TomoSAR imaging, which is based on the following equation

$$\mathrm{P}(y,x,z)=\left|\frac{1}{\sqrt{N}}\sum_{n=1}^{N}SLC_n\left(r_n(y,z),x\right)e^{-j\frac{4\pi}{\lambda}r_n(y,x,z)}\right|^2 \quad (2)$$

Where: o P(y, x, z) is the tomographic backscattered power at ground range-azimuth location (y, x) and at z meters above the terrain level; o y represents the ground-range coordinate; o r_n(y, x, z) represents the (zero-Doppler) distance between the n-th trajectory and a generic target at (y, x, z).

SAR back-projection considers the real 3-D imaging geometry by interpolating the returned signals as well as compensating for the phase term of the actual distance between sensor system and object target. This is more appropriate when considering the case of high resolution airborne SAR systems, for which image coregistration can significantly depends on height [10-11, 16]. Moreover, the phase calibration processing [12-13], which is necessary to mitigate the impact of propagation disturbances, was implemented before performing SAR back-projection algorithm.

2.3 RELATING SAR TOMOGRAPHY TO AGB VIA LIDAR DATA

With available in-situ measurements, a linear relationship can be built between AGB and TomoSAR backscattered power at a certain layer above the ground by the following log law

$$10\lg(P)=a\cdot AGB+b \quad (3)$$

Where a and b are two parameters to be fitted for the line, P is the TomoSAR backscattered power. Fig. 2 shows the HV polarization backscattered power for three different layers above the ground and their corresponding relationships to the in-situ measurements. From Fig. 2, the best correlation could be found at the layer centered at 30 m, which is consistent with the results shown in previous studies [5-6].

Fig. 3 shows the LiDAR derived AGB and the comparison between LiDAR derived AGB and in-situ measurements. As we can see, saturation problem could be found for high level LiDAR AGB higher than 400 ton/ha.

Fig. 4 represents the joint distribution between tomographic power and LiDAR derived AGB. From the figure we can clearly see that there exists a linear relationship when LiDAR AGB ranges from about 270 ton/ha to 400 ton/ha, whereas the saturation problem emerges again at higher AGB level. As a result, the parameters a and b that link tomographic power to AGB are estimated by considering LiDAR AGB only in the range between 270 ton/ha and 400 ton/ha, see Fig. 5 (a). Final retrieval performance was validated by evaluating the root mean square error (RMSE) between in-situ AGB and the retrieved AGB, which is shown in Fig. 5 (b). The overall RMSE for the sixteen plots was 23.27 ton/ha, i.e., 6.55% in

percentage. For in-situ AGB higher than 400 ton/ha, a slight underestimation of AGB can be observed, which is in accordance with the saturation problem characterized in Fig. 4.

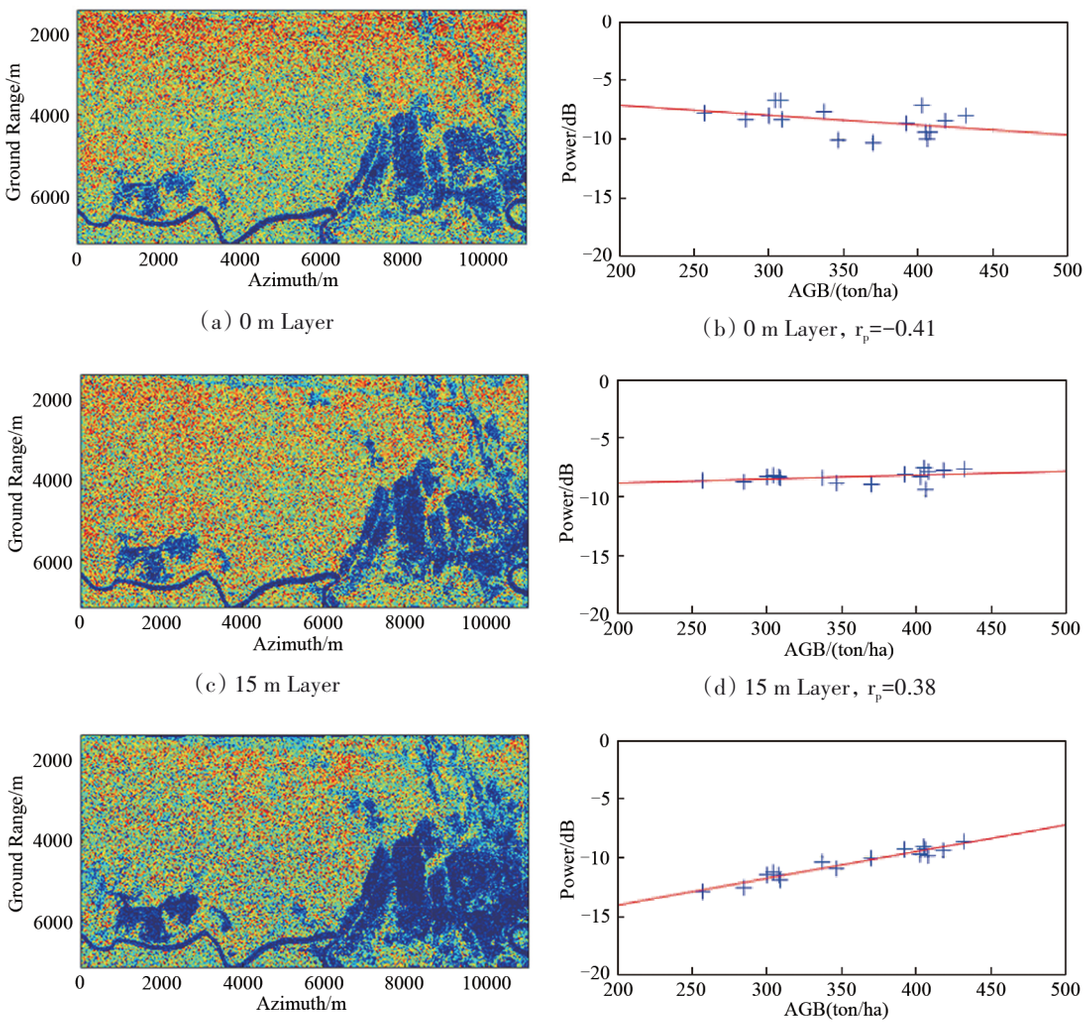

(a) 0 m Layer (b) 0 m Layer, r_p=−0.41

(c) 15 m Layer (d) 15 m Layer, r_p=0.38

(e) 30 m Layer (f) 30 m Layer, r_p=0.97

Fig.2 Tomographic power at (a) 0 m, (c) 15 m, (e) 30 m layer above the ground. Tomography is here implemented using 7 passes. Linear correlation between in-situ measurements and tomographic power at (b) 0 m, (d) 15 m, (f) 30 m layer above the ground.

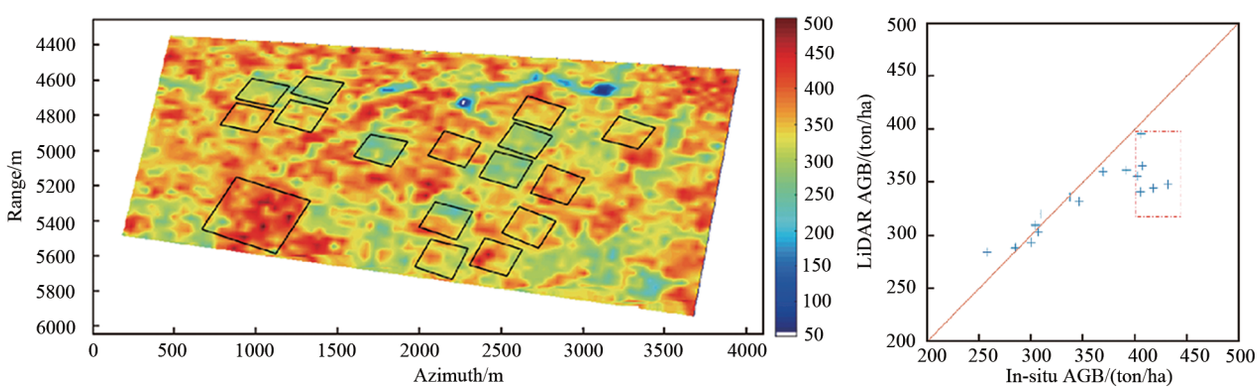

(a) LiDAR AGB/(ton/ha) (b) RMSE=37.7 ton/ha=10.61%

Fig.3 (a) LiDAR derived AGB; (b) Comparison between in-situ AGB and LiDAR derived AGB.

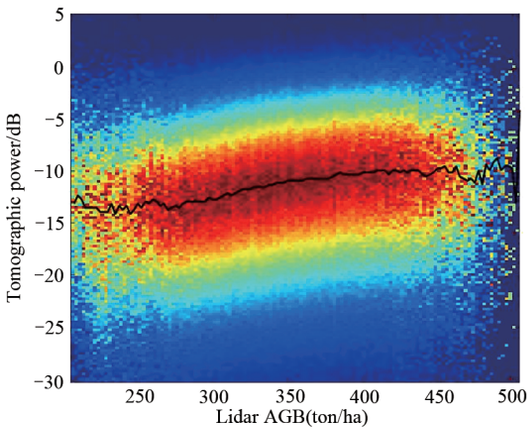

Fig.4 Joint distribution between tomographic power at 30 m layer and LiDAR derived AGB. The distribution has been normalized that the maximum is unitary along each column. The black line connects the mode value for each column. Picture drawn from [16]

3 IMPACT OF CHANGING WEATHER CONDITIONS ON BIOMASS TOMOGRAPHY

3.1 TROPISCAT DATA SET

TropiSCAT was implemented as a P-band fully polarimetric ground-based campaign in the tropical rain forest area of Paracou, French Guiana [14]. The system consists of 20 antennas installed on the 55-m high Guyaflux tower to form an equivalent monostatic vertical array of 15 elements for each polarization. The system was operated to collect tomographic data every 15 minutes [14].

The data analyzed in this paper are those acquired at 06:00 a.m., consistently with BIOMASS acquisition plan. The analyzed dataset covers a time span from December 6, 2011 to February 29, 2012.

3.2 BIOMASS TOMOGRAPHY SIMULATION

To mimic BIOMASS tomograms, tomographic imaging is performed by using acquisitions gathered on different days, instead of using simultaneous acquisitions as in [14]. BIOMASS tomography will be implemented by taking 7 acquisitions with a time separation of three days from one another. Therefore, tomograms are obtained by using the signals gathered from two TropiSCAT antennas every three days and from three antennas on the last day, so that the collection of data at all 15 antennas is spread over 7 different days, for a total period of 18 days. We will hereafter refer to these tomograms as "7-day Tomograms". Fig. 6 shows 4 7-day Tomograms under different weather conditions. Each 7-day Tomogram is associated with an "Instantaneous Tomogram" obtained by taking all 15 antennas at 6:00 AM on the 7th day, which is used as reference.

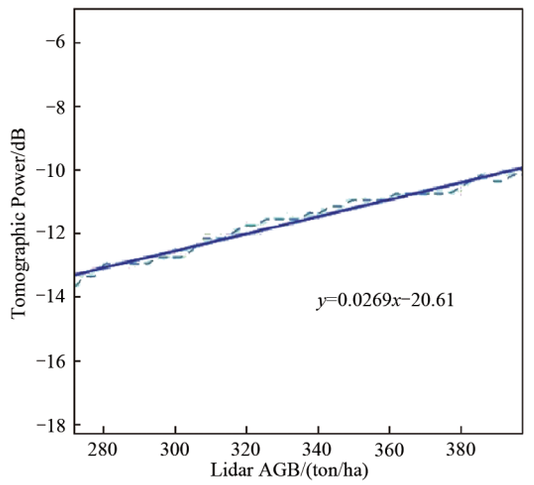

(a) Fitted linear relationship between tomographic power and LiDAR derived AGB

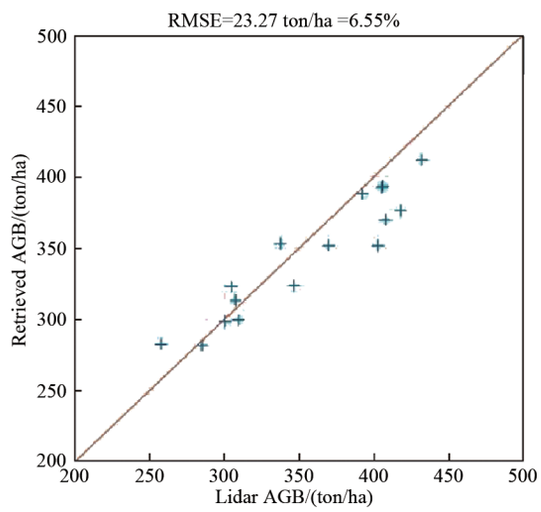

(b) Comparison between in-situ AGB and retrieved AGB from the fitted line. Picture drawn from [16]

Fig.5

3.3 INTENSITY TIME SERIES

The intensity time series across all the 63 7-day Tomograms has also been studied. The relative intensity variation is quantified as:

$$\sigma_{\text{rel}} = 10lg10\left(\frac{\bar{P}_7}{\bar{P}_7 + \sigma}\right) \tag{4}$$

Where σ and $\bar{P}_7$ are the standard deviation and the average of the backscattered power of 63 7-day Tomograms. Fig. 7 shows the intensity variation of all the 7-day Tomograms at HH, VH and VV channel.

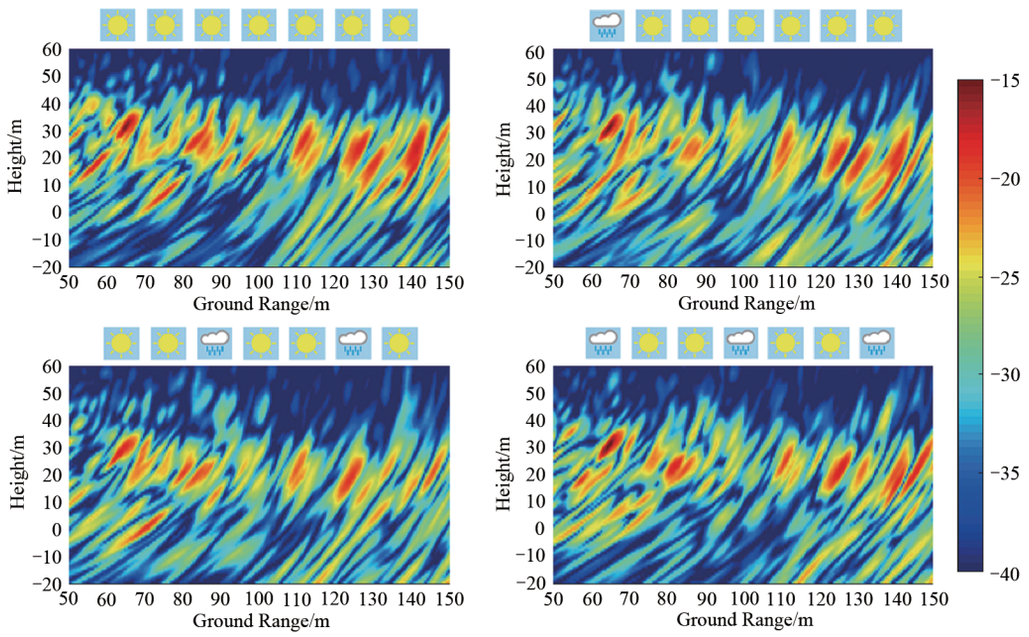

Fig.6 7−day Tomograms acquired under different weather conditions. The distribution of sunny and rainy days is shown in the graphics above each panel. Picture drawn from [17].

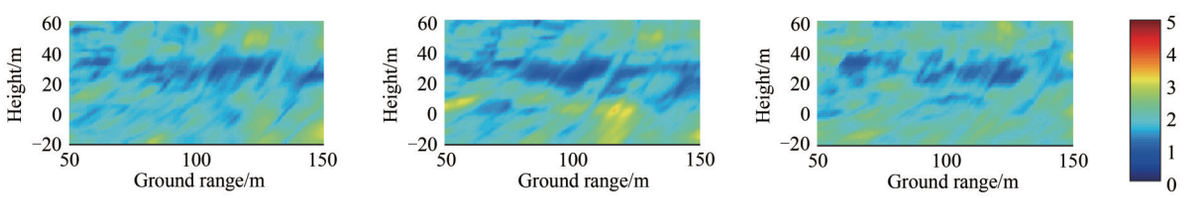

(a) HH (b) VH (c) VV

Fig.7 Intensity variations of 7−day Tomograms. Units are in dB. Picture drawn from [17].

4 DISCUSSION AND CONCLUSIONS

This work has provided an empirical assessment of the possibility to use LiDAR data to train AGB retrieval based on P-Band SAR tomography in tropical forests. Although quite preliminary, the results support the idea that LiDAR and SAR Tomography could greatly benefit each other, so that the advantages of SAR tomography, e.g. high sensitivity to AGB and continuous coverage, could be effectively transformed to accurate AGB maps by using relatively few LiDAR measurements.

Moreover, the impact of changing weather conditions on BIOMASS tomography was investigated by mimicking BIOMASS tomography using TropiSCAT data. Based on intensity time series, the variation of the tomographic signal at canopy level can be assessed in about 1—1.5 dB r.m.s. (1 sigma) in cross-polarization. This can be transposed into a biomass estimation error by considering that at this forest site tomographic intensity at 30 m was observed to increase about 4 dB as forest biomass passes from 250 to 450 tons per hectare [5-6], see also Fig.2 (f). Accordingly, the observed variation of 1—5 dB in the 7-day Tomograms would entail a biomass retrieval error of around 50—80 tons per hectare at this test site using tomography, which is on the order about 20% or better.

REFERENCES

SaatchiS. S., HarrisN. L., BrownS., et al., "Benchmark map of forest carbon stocks in tropical regions across three continents," Proceedings of the National Academy of Sciences., vol. 108, no. 24, pp. 9899-9904, Jun. 2011.

PanY., BirdseyR. A., FangJ., et al., "A large and persistent carbon sink in the world's forests, Science", vol. 333, no. 6045, pp. 988-993, Aug. 2011.

Le ToanT., QueganS., DavidsonM., BalzterH., PaillouP., PapathanassiouK., PlummerS., RoccaF., SaatchiS., ShugartH., and UlanderL., "The BIOMASS mission: Mapping global forest biomass to better understand the terrestrial carbon cycle," Remote Sens. *Environ.*, vol. 115, no. 11, pp. 2850 – 2860, Nov. 2011.

ESA (2012, Report for mission selection: biomass, Noordwijk, The Netherlands, 2012.

D. Ho Tong Minhet al., "Relating P-band synthetic aperture radar tomography to tropical forest biomass," IEEE Trans. Geosci. Remote Sens., vol. 52, no. 2, pp. 967 – 979, Feb. 2014.

Ho Tong MinhD., Le ToanT., RoccaF., TebaldiniS., VillardL., Re´jouMe´chainM., PhillipsO. L., Feld- pauschT. R., Dubois-FernandezP., ScipalK. et al., "SAR tomography for the retrieval of forest biomass and height: Cross-validation at two tropical forest sites in French Guiana," Remote Sens. Environ. vol. 175, pp. 138 – 147, Mar. 2016.

Dubois-FernandezP. C., Le ToanT., DanielS., OriotH., ChaveJ., BlancL., VillardL., DavidsonM. W. J., and PetitM., "The TropiSAR airborne campaign in French Guiana: Objectives, description, and observed temporal behavior of the backscatter signal," IEEE Trans. Geosci. Remote Sens., vol. 50, no. 8, pp. 3228 – 3241, Aug. 2012.

Reigber and AA.. Moreira, "First demonstration of airborne SAR to-

mography using multibaseline L-band data," *IEEE Trans*. Geosci. Remote Sens., vol. 38, no. 5, pp. 2142–2152, Sep. 2000.

GiniF., LombardiniF., and MontanariM., "Layover solution in multibaseline SAR interferometry," IEEE Trans. Aerosp. Electron. Syst., vol. 38, no. 4, pp. 1344–1356, Oct. 2002.

FreyO., MagnardC., Ruegg and EM.. Meier, "Focusing of Airborne Synthetic Aperture Radar Data From Highly Nonlinear Flight Tracks," *IEEE Trans*. Geosci. Remote Sens., vol. 47, no. 6, pp. 1844-1858, Jun. 2009.

Tebaldini S., Nagler T., Rott H., Heilig A., Imaging the Internal Structure of an Alpine Glacier via L-Band Airborne SAR Tomography, 2016) IEEE Transactions on Geoscience and Remote Sensing, 54 (12), pp. 7197-7209, Dec. 2016.

Tebaldini and AS.. Guarnieri, "On the role of phase stability in SAR multibaseline applications," *IEEE Trans*. Geosci. Remote Sens., vol. 48, no. 7, pp. 2953–2966, Jul. 2010.

TebaldiniS., RoccaF., Mariotti d'AlessandroM., and Ferro-FamilL., "Phase calibration of airborne tomographic SAR data via phase center double localization," IEEE Trans. Geosci. Remote Sens., vol. 54, no. 3, pp. 1775–1792, Mar. 2016.

Ho Tong MinhD., TebaldiniS., RoccaF., KoleckT., BorderiesP., AlbinetC., VillardL., HamadiA., and Le ToanT., "Ground-based array for tomographic imaging of the tropical forest in P-band," IEEE Trans. Geosci. Remote Sens., vol. 51, no. 8, pp. 4460–4472, Mar. 2013.

Ho Tong MinhD., TebaldiniS., RoccaF., Le ToanT., BorderiesP., KoleckT., AlbinetC., HamadiA., and VillardL., "Vertical structure of p-band temporal decorrelation at the paracou forest: Results from tropiscat," IEEE Geosci. and Remote Sens. Lett., vol. 11, no. 8, pp. 1438–1442, Aug. 2014.

YangX., D'AlessandroM. M., TebaldiniS., M. Liao "Relating Sar Tomography to Tropical Forest Biomass via Lidar Data", IGARSS 18, Valencia, 2018.

BaiY., TebaldiniS., Minh and WD. H. T.. Yang, "An Empirical Study on the Impact of Changing Weather Conditions on Repeat-Pass SAR Tomography," in IEEE Journal of Selected Topics in Applied Earth Observations and Remote Sensing, doi: 10.1109/JSTARS.2018.2818796